Original article
Section: Food Quality and Functionality

Physicochemical and Sensory Properties with Special Emphasis on Thermal Characteristics of Whey Butter from Gouda Cheese Production Compared to Milk Butter

Oskar Michał Brożek* , Katarzyna Kiełczewska , Krzysztof Bohdziewicz

*Department of Dairy Science and Quality Management, Faculty of Food Sciences,
University of Warmia and Mazury in Olsztyn, Oczapowskiego Str. 7, 10–719 Olsztyn, Poland*

The aim of this study was to characterise milk fat from whey butter and to identify potential differences between whey butter (WB) and sweet cream butter (milk butter – MB). The fatty acid (FA) profile, thermal properties, colour parameters, texture properties, and sensory attributes of MB and WB were compared. The values of texture properties (firmness, brittleness, and cohesiveness) and colour parameters (values of b^* and the yellowness index) of WB were lower than MB. The sensory analysis showed lower values of consistency descriptors (firmness, brittleness, cohesiveness), a less intense nutty and milky aroma, and a more intense cheesy aroma and taste in WB than in MB. WB was more abundant in monounsaturated, polyunsaturated, and long-chain FAs, including C18:0, C18:1 Σt, C18:1 Σc, C18:2, C18:3, and C18:2 $c9$, $t11$, and it was less abundant in saturated and medium-chain FAs, including C10:0, C12:0, C14:0, C14:1, C15:0, C16:0, and C16:1, relative to MB. Water content (MB vs WB and the corresponding fats) and thermal history (single vs repeated heating and cooling treatments) affected differential scanning calorimetry curves and phase transition peaks. The principal component analysis revealed that the FA profile influenced the crystallisation and melting peaks of MB fat (MBF) and WB fat (WBF). WBF crystallisation occurred at a lower temperature, was characterised by lower enthalpy, and proceeded more rapidly than MBF crystallisation. Various fat fractions had different melting characteristics, and most WBF fractions were characterised by lower melting enthalpy and a smaller maximum difference in heat flow than MBF. Whey butter and milk butter differed in physicochemical properties and sensory attributes, and their thermal profiles depended on the FA profile, water content, and thermal history.

INTRODUCTION

The coagulation of milk proteins in cheesemaking leads to the separation of milk components into two phases: curd and whey. Around 8 to 9 kg of whey is generated in the production of 1 kg of cheese. The global production of whey is estimated at 165 million tons, and it continues to increase by 1–2% every year [Panghal *et al.*, 2018]. Whey obtained during cheesemaking is utilised in 75% in Europe and in less than 50% on other continents [Macwan *et al.*, 2016]. Different types of whey are obtained in various cheese production technologies. Sweet whey is the by-product of rennet coagulation of milk, whereas acid whey is obtained during acid coagulation of milk. Sweet and acid whey differ in composition and parameters that determine their suitability for further processing [Nishanthi *et al.*, 2017]. Depending on the cheesemaking technology, 50–60% of milk solids are transferred to whey. Some of the separated solids have very high nutritional value. When whey is further processed (into whey protein concentrate, lactose, lactic acid), residual fat is separated from other components [Kasapcopur *et al.*, 2021; Macwan

et al., 2016]. Some fat is transferred to whey during cheesemaking. Concentrated whey fat in the form of whey cream can be processed into various products, such as whey butter [Jinjarak *et al.*, 2006; Panghal *et al.*, 2018].

The composition of milk fat is influenced by numerous factors, including seasonal variations, animal nutrition, lactation phase, and technology of dairy products. Differences in milk fat composition affect the physicochemical properties of butter [Amal, 2009; Anankanbil *et al.*, 2018; Couvreur *et al.*, 2006].

The phase transitions of milk fat, especially crystallisation and melting (which occur within a temperature range of –40°C to 40°C), are mainly affected by the physicochemical properties of fat, including the fatty acid (FA) profile, fat crystal structure, and the size of fat globules [Hokkanen *et al.*, 2021; Michalski *et al.*, 2004; Truong *et al.*, 2014]. The crystallisation of anhydrous milk fat was reported to differ between the hard (with a higher content of C14:0, C16:0, C18:0) and soft (with a higher content C18:1) milk fat fractions [Truong *et al.*, 2014]. Milk fat can be divided into three fractions based on melting temperature: the low-melting point

---

408

Pol. J. Food Nutr. Sci., 2022, 72(4), 407–419

fraction (LMPF) with a melting temperature below 10°C, the middle-melting point fraction (MMPF) with a melting temperature of 10–25°C, and the high-melting point fraction (HMPF) with a melting temperature higher than 25°C. The melting process of each fraction is represented by distinct endothermic peaks on differential scanning calorimetry (DSC) curves [Anankanbil *et al.*, 2018; Brożek *et al.*, 2022a, b; Hokkanen *et al.*, 2021]. The FA profile of milk fat, in particular the triacylglycerol (TAG) profile, determines the melting temperature of LMPF, MMPF, and HMPF, and influences the rheological properties of butter [Omar *et al.*, 2017]. According to Anankanbil *et al.* [2018], a high content of C14:0 and C16:0 increased the melting temperature of MMPF and HMPF, whereas a high content of C18:0, C18:1, and C18:2 decreased melting temperature. A higher C16:0/C18:1 ratio significantly increased the melting temperature of milk fat and butter firmness [Couvreur *et al.*, 2006]. Milk fat melting is a complex process due to the presence of three polymorphic crystal forms of fat with different properties and crystalline structure. The hexagonal α form (the least stable form that undergoes reversible crystallisation during rapid cooling) can be irreversibly transformed to a β' (more stable orthorhombic form) and β form (the most stable triclinic form) [Fredrick *et al.*, 2011; Hondoh & Ueno, 2016; Lopez & Ollivon, 2009; Staniewski *et al.*, 2021; Viriato *et al.*, 2019]. The thermal history of milk fat, which is determined during successive heating and cooling treatments, illustrates changes in the polymorphic structure of crystals and can be used to determine differences in melting behaviour relative to fat that was not subjected to thermal treatment. The thermal history of dairy products is recorded during thermal treatments, such as cream aging in butter production. Thermal history affects the ratio of solid to liquid fat phases, thus influencing the rheological properties of butter [Jukkola & Rojas, 2017; Staniewski *et al.*, 2021].

Milk and dairy products are complex matrices, where each component is characterised by unique phase transformations. In the results of DSC analysis, the phase transition peaks of different components can overlap if they occur within a similar temperature range. The above influences the identification of phase transition peaks in DSC curves and the corresponding peak parameters [Amara-Dali *et al.*, 2007; Lopez *et al.*, 2005; Tomaszewska-Gras, 2013]. Examples of overlapping phase transition peaks include fat crystallisation and melting peaks, and water freezing and ice melting peaks. Therefore, the presence of water in butter can significantly affect the observed phase transition peaks of butter fat in DSC curves. In DSC analyses, more complex thermal properties of milk fat can be observed in butter samples that do not contain water or have reduced water content than in butter samples with standard water content.

The aim of this study was to characterise milk fat from butter made from whey which was obtained from Gouda cheese production, and to identify potential differences between whey butter (WB) and sweet cream butter (milk butter – MB). The following research hypotheses were formulated: 1) MB and WB do not differ in selected physicochemical properties or sensory attributes; 2) the thermal profile of butter is not influenced by the type of butter, FA profile, presence of water or thermal history (DSC analysis of single *vs* multiple heating and cooling treatments). The research hypotheses were validated by measuring the FA profile, thermal properties, colour parameters, texture properties, and sensory attributes of MB and WB.

MATERIALS AND METHODS

Research materials

MB and WB were obtained from a dairy plant (Spółdzielnia Mleczarska Rospuda in Filipów, Warmia and Mazury voivodeship, Poland) as the final products of periodic churning performed under the same industrial conditions. WB was produced from whey obtained from Gouda cheese production. MB was produced from sweet milk cream. MB and WB were collected in triplicate during the week from different batches in the amount of 1 kg (*n*=3).

Water was removed from MB and WB to determine its influence on the thermal characteristics of fat. Butters were clarified at 60°C; the fat phase was separated from the aqueous phase, and the fat phase was filtered through filter paper containing anhydrous sodium bisulphate roasted at a temperature of 150°C. The above procedure was applied to obtain milk butter fat (MBF) and whey butter fat (WBF). The samples of MBF and WBF were obtained from one clarification process for each sample.

Samples of MB and WB were analysed for chemical composition, FA profile, colour parameters, texture properties, and sensory attributes. Samples of MB, WB, MBF, and WBF were used in the DSC analysis.

Chemical composition analysis

The content of total solids, solids-non-fat, and water of WB and MB was determined with the FoodScan Dairy Analyser (Foss, Hillerød, Denmark). Fat content was determined with the gravimetric method by Rose-Gottlieb according to ISO 1211 [ISO, 2010].

Fatty acid profile analysis

Extraction of milk fat was conducted by the Rose-Gottlieb method [ISO, 2010]. Fatty acid esters were prepared according to ISO 15884 [ISO, 2002]. The 7890A gas chromatograph with a flame ionisation detection (Agilent Technologies, Santa Clara, CA, USA) was used to determine the FA profile on the CP-Sil 88 column (100 m × 0.25 mm, 0.20 μm; Agilent Technologies) with a thermal gradient from 60°C (1 min) to 180°C at 5°C/min; injector and detector temperature, 225°C and 250°C, respectively; flow rate of carrier gas (helium), 0.8 mL/min; split ratio, 1:50; injection volume, 1 μL; liner, 0.4 mm. The reference material was BCR-164 anhydrous milk fat (LGC Standards, Kiełpin, Poland). The proportions of fatty acids were calculated and divided into the following groups: saturated fatty acids (SFAs), monounsaturated fatty acids (MUFAs), polyunsaturated fatty acids (PUFAs), short-chain fatty acids (SCFAs; C4–C8), medium-chain fatty acids (MCFAs; C10–C15), long-chain fatty acids (LCFAs; C16–C19), and branched-chain fatty acids (BCFAs; C13:0 *i*, C13:0 *ai*, C14:0 *i*, C15:0 *i*, C15:0 *ai*, C16:0 *i*). The following abbreviations were used in the description of fatty acid isomers: *ai* – *anteiso*, *i* – *iso*, *c* – *cis*, *t* – *trans*.

Differential scanning calorimetry analysis

The Q10 DSC analyser with a closed refrigerated cooling system (TA Instruments, New Castle, DE, USA) was calibrated with indium. The DSC analysis (sample weight: 10 ± 1 mg; type of measuring crucibles: biconvex hermetically sealed aluminium crucible; gas: nitrogen; flow rate: 50 mL/min, reference sample: empty crucible) was divided into two consecutive and uninterrupted cycles to determine the influence of the thermal history of butter and butter fat on the melting behaviour of milk fat. In the first cycle, measurements were conducted in the following sequence: I – heating from –40°C to 95°C, II – cooling from 95°C to –40°C. The sequences from the first cycle were repeated three times in the second cycle. In each stage, temperature was changed at a rate of 10°C/min, and at the end of each stage, the samples were maintained at the final temperature for 1 min. The results of the DSC analysis were processed in the Universal Analysis 2000 program (TA Instruments). The following parameters of the identified phase transition peaks were determined according to Brożek *et al.* [2022b]: maximum peak temperature (T_{max}), phase transition onset temperature (T_{onset}), transition temperature range as peak width at half height ($\Delta T_{1/2}$), enthalpy (ΔH), peak height at maximum (P_{height}), starting (P_s) and ending (P_e) points of the peak.

Colour analysis

The colour analysis was performed in the CIELab space. Three colour parameters were measured: L^*, lightness from black (0) to white (100); a^*, greenness (–) to redness (+); b^*, blueness (–) to yellowness (+) with the CR-400 Chroma Meter (Konica Minolta Sensing Americas, Inc., Ramsey, NJ, USA) calibrated against a white plate (L^*=95.42; a^*=4.89 and b^*=–2.43). The results were used to calculate chromaticity (C^*), the whiteness index (WI), and the yellowness index (YI) according to equations (1), (2), and (3), respectively.

$$C^* = (a^{*2} + b^{*2})^{1/2} \qquad (1)$$

$$WI = 100 - [(100 - L^*)^2 + a^{*2} + b^{*2}]^{1/2} \qquad (2)$$

$$YI = 142.86\, b^*/L^* \qquad (3)$$

The total difference in colour chroma (ΔC^*) between MB and WB was calculated with the use of formula (4), and the total difference in colour (ΔE) between MB and WB was calculated with the use of formula (5).

$$\Delta C^* = C_{MB}^{*2} - C_{WB}^{*2} \qquad (4)$$

$$\Delta E = [(L_{MB}^* - L_{WB}^*)^2 + (a_{MB}^* - a_{WB}^*)^2 + \\ + (b_{MB}^* - b_{WB}^*)^2]^{1/2} \qquad (5)$$

All parameters were calculated according to Pathare *et al.* [2013].

Texture analysis

Instrumental texture analyses were conducted with the use of the TA.XT.plus Texture Analyser (Stable Micro Systems, Godalming, United Kingdom) with Texture Exponent

32 software. Butter samples were stored in a refrigerator at 6 ± 1°C, and texture analyses were conducted at the same temperature in the micro thermostatic chamber (Temperature Applied Sciences Ltd, West Sussex, United Kingdom) cooled with liquid nitrogen from the XL-120 cylinder (Taylor-Wharton Gas Equipment Sdn. Bhd., Shah Alam, Selangor, Malaysia). The sample was positioned centrally under a P/6 cylindrical flat probe. Butter firmness (N), consistency (N×s), cohesiveness (N), and the viscosity index (N×s) were determined in a penetration test (speed: 2 mm/s; distance: 20 mm). Firmness was measured as the maximum force needed to press the probe into the sample. Cohesiveness was described as the maximum force needed to overcome the resistance of the sample when the probe returns to its initial position. Consistency and the viscosity index were expressed by the area under the force *vs* time curve when the probe penetrated the sample and returned to its initial position, respectively. Butter cohesiveness and the viscosity index were described by negative values, and they were related to the direction of probe movement [Sánchez & Pérez, 2012; Tarapata *et al.*, 2021].

Sensory evaluation

The sensory profiles of MB and WB were determined on a descriptive scale according to ISO 13299 [ISO, 2016]. The evaluation was conducted by a panel of eight trained specialists with confirmed taste sensitivity according to ISO 8586 [ISO, 2014]. The descriptors were selected by the panel. Each panellist received a product sheet and a score sheet. The following quality descriptors were considered in the evaluation: appearance (1 descriptor – colour uniformity), aroma (4 descriptors – milky, pasteurisation, nutty and cheesy aroma), consistency (3 descriptors – firmness, cohesiveness, brittleness), and taste (4 descriptors – milky, pasteurisation, nutty and cheesy). Sensory attributes were evaluated on a five-point descriptive scale (1 to 5 points). The intensity of each sensory attribute was determined (1 – absence of descriptor, 5 – very intense).

Statistical analysis

The results of fatty acid profile, colour parameters, texture properties, and sensory attributes for MB and WB were analysed with the Student's *t*-test ($p\leq0.05$). One-way ANOVA (normal distribution was verified using the Shapiro-Wilk test) was performed for the results of thermal properties, and the significance of differences between means was determined in Duncan's test at α=0.05. The relationship between the percentage content of individual FAs in total FAs in each sample and parameters of phase transition peaks was determined by principal component analysis (PCA). Data were processed statistically in StatSoft Inc. Statistica v. 13.1 software (Tulsa, OK, USA).

RESULTS AND DISCUSSION

In MB, the content of total solids was 85.20 ± 0.03 g/100 g, solids-non-fat – 1.41 ± 0.16 g/100 g, fat – 83.94 ± 0.06 g/100 g, and water – 14.93 ± 0.08 g/100 g. In WB, the content of total solids was 85.87 ± 0.08 g/100 g,

solids-non-fat – 1.52±0.09 g/100 g, fat – 84.56±0.06 g/100 g, and water – 14.27±0.09 g/100 g. The obtained results were consistent with the values of Food and Agriculture Organization/World Health Organization standard [FAO/WHO, 2018] and the values given in the literature [Kasapcopur *et al.*, 2021; Nadeem *et al.*, 2014].

Fatty acid profile

An analysis of the FA profile revealed that C14:0, C16:0, C18:0, and C18:1 Σ*c* FAs dominated and accounted for 75.44 and 78.25 g/100 g of total FAs in WB and MB, respectively (Table 1). The remaining FAs were detected in smaller quantities. Samples of MB and WB differed significantly ($p \leq 0.05$) in the proportions of most FAs. Whey butter was significantly ($p \leq 0.05$) more abundant in C4:0, C15:0 *i*, C15:0 *ai*, C17:1, C18:0, C18:1 Σ*t*, C18:1 Σ*c*, C18:2, C18:3, C18:2 *c*9, *t*11, MUFAs, PUFAs, SCFAs, and LCFAs, but less abundant in C10:0, C10:1, C12:0, C13:0 *i*, C13:0 *ai*, C13:0, C14:0, C14:1, C15:0, C16:0 *i*, C16:0, C16:1, SFAs, and MC-FAs than MB. The FA profiles of both products were typical of MB and WB [Gómez-Mascaraque *et al.*, 2020; Nadeem *et al.*, 2014; Staniewski *et al.*, 2021].

The observed differences in the FA profiles of WB and MB probably resulted from the whey origin or whey cream production technology. The production of whey cream involves a larger number of processing operations than the production of milk cream, which promotes changes in milk fat globules (MFG) and milk fat globule membrane (MFGM) components in whey cream [Brighenti *et al.*, 2021; Jukkola & Rojas, 2017]. The FA profiles of whey depend on the cheese from which whey originates. WB was obtained from the whey of Gouda cheese, which is commonly produced in Europe. The available literature provides only reports from the studies of whey butter produced from the whey of regional cheeses or experimental products; therefore, some differences could be noticed between the FA profile of WB in the present study and the works of other authors. Çetinkaya [2021] found a higher percentage of unsaturated fatty acids (UFAs) in whey fat (from Kashar cheese) than in milk fat, but Kasapcopur *et al.* [2021] found no differences between whey fat (a mixture of whey from rennet-coagulated White-brined and Kashar and acid-coagulated Lor cheeses) and milk fat in the content of UFAs. Brighenti *et al.* [2021] reported greater differences in the size of MFG and a higher content of phospholipids in whey cream from soft cheese (Munster) than in milk cream. They observed that MFGM could be damaged during cheesemaking and whey processing operations, which can promote the formation of larger MFG aggregates. The FA profile of the MFG core differs from the FA profile of MFGM. The FA composition of MFGM phospholipids is characterised by a higher content of UFAs than the FA composition of core TAGs [Jhanwar & Ward, 2014]. According to Fauquant *et al.* [2005], MFGM are more abundant in UFAs, in particular PUFAs whose content is approximately six times higher than in the MFG core. Based on these studies, it can be assumed that the higher content of UFAs-rich phospholipids in WB compared to MB was responsible for the different FA profile in MB and WB, but this requires further studies.

TABLE 1. Fatty acid profile of milk butter and whey butter (g/100 g total fatty acids).

Fatty acid	Milk butter	Whey butter
C4:0	2.14±0.07[b]	2.78±0.12[a]
C6:0	1.72±0.08[a]	1.81±0.02[a]
C8:0	1.11±0.01[a]	1.13±0.02[a]
C10:0	2.65±0.04[a]	2.56±0.03[b]
C10:1	0.33±0.02[a]	0.28±0.01[b]
C11:0	0.02±0.01[a]	0.02±0.01[a]
C12:0	3.31±0.07[a]	3.06±0.05[b]
C12:1	0.05±0.01[a]	0.02±0.01[a]
C13:0 *i*	0.11±0.01[a]	0.04±0.01[b]
C13:0 *ai*	0.10±0.01[a]	0.08±0.01[b]
C13:0	0.11±0.01[a]	0.09±0.01[b]
C14:0 *i*	0.15±0.02[a]	0.14±0.01[a]
C14:0	12.03±0.17[a]	10.79±0.14[b]
C14:1	1.31±0.03[a]	0.93±0.01[b]
C15:0 *i*	0.28±0.01[b]	0.33±0.01[a]
C15:0 *ai*	0.46±0.01[b]	0.57±0.02[a]
C15:0	1.36±0.05[a]	1.19±0.02[b]
C16:0 *i*	0.29±0.01[a]	0.28±0.01[b]
C 16:0	36.20±0.53[a]	30.61±0.92[b]
C16:1	2.11±0.07[a]	1.67±0.05[b]
C17:0	0.61±0.06[a]	0.64±0.02[a]
C17:1	0.14±0.02[b]	0.25±0.02[a]
C18:0	9.71±0.32[b]	11.33±0.44[a]
C18:1 Σ*t*	1.13±0.16[b]	3.31±0.14[a]
C18:1 Σ*c*	20.31±0.34[b]	22.71±0.69[a]
C18:2 Σ*t*	0.11±0.03[a]	0.07±0.01[a]
C18:2	1.16±0.03[b]	1.23±0.09[a]
C18:2 *c*9, *t*11	0.38±0.03[b]	1.08±0.04[a]
C18:3	0.50±0.02[b]	0.88±0.02[a]
C19:0	0.12±0.02[a]	0.11±0.04[a]
SFA	72.48±0.45[a]	67.57±0.78[b]
MUFA	25.37±0.22[b]	28.18±0.37[a]
PUFA	2.27±0.07[b]	4.38±0.12[a]
SCFA	4.97±0.21[b]	5.72±0.08[a]
MCFA	22.26±0.23[a]	20.10±0.11[b]
LCFA	72.89±0.29[b]	74.30±0.44[a]
BSFA≤C16	1.39±0.02[a]	1.44±0.03[a]

Values are means ± standard deviations ($n=3$); values with different superscripts in row differ significantly at $p \leq 0.05$. *i*– iso; *ai* – anteiso; *c* – cis; *t* – trans; SFA – saturated fatty acids; MUFA – monounsaturated fatty acids; PUFA – polyunsaturated fatty acids; SCFA – short-chain fatty acids (C4–C8); MCFA – medium-chain fatty acids (C10–C15); LCFA – long-chain fatty acids, (C16–C19); BSFA – branched saturated fatty acids (C13:0 *i*, C13:0 *ai*, C14:0 *i*, C15:0 *i*, C15:0 *ai*, C16:0 *i*).

Differential scanning calorimetry (DSC)

The shape of DSC curves differed subject to butter type, water content, and the sample's thermal history (Figure 1, Figure 2, Figure 3). These differences affected the parameters of phase transition peaks describing both exothermic (Table 2) and endothermic (Table 3) transitions. Butter samples and the corresponding fat samples were compared to determine which phase transition peaks correspond to changes in milk fat and water. MBF and WBF were also used in the analysis to minimise differences in the fat content of samples which could have influenced the shape of DSC curves and the parameters of phase transition peaks.

The DSC curves plotted for MBF and WBF had a similar shape, but differed from the curves generated for MB and WB due to the presence of water in the analysed samples (Figure 1). The phase transitions of water in the butter samples (water freezing, ice melting, evaporation) induced much greater changes in heat flow than the phase transitions of fat. Phase transitions of water were visualised by large peaks in DSC curves (Figure 1, Figure 2, Figure 3). These peaks overlapped the peaks representing the phase transitions of milk fat, in particular endothermic peaks associated with fat melting (Figure 2). The parameters of crystallisation and ice melting peaks are consistent with those given in the literature [Tomaszewska-Gras, 2012].

Two exothermic peaks were observed in DSC curves in the range of –40°C to 16.5°C during cooling from 95°C to –40°C. A first peak (A) occurred in all samples between around –40°C to around 14°C, and a second peak (B) occurred between around 10°C to around 15°C (Figure 2).
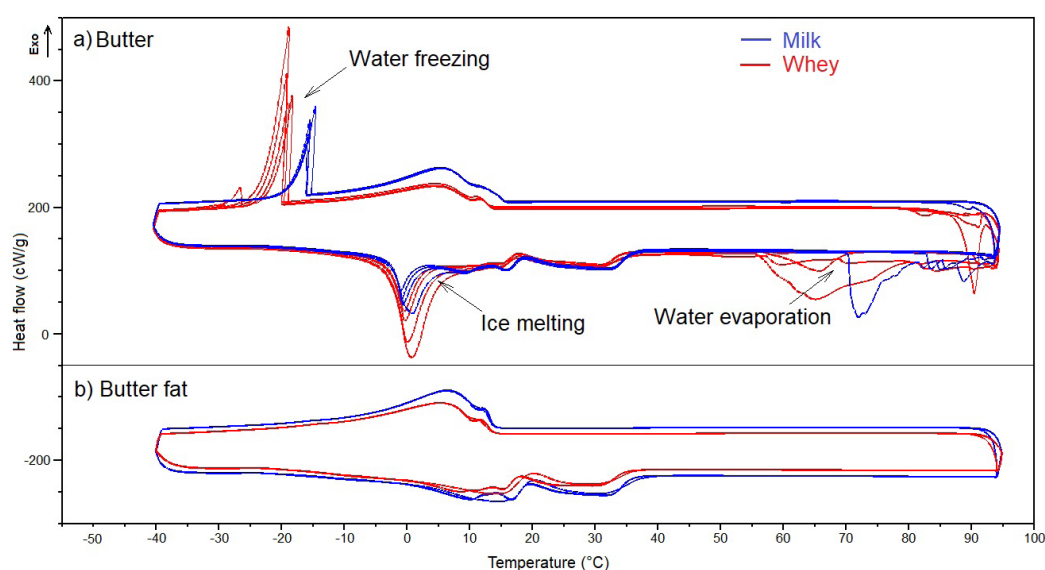

FIGURE 1. Differential scanning calorimetry (DSC) curves of milk butter and whey butter (a) and the corresponding fats (b) with an indication of the phase transitions of water, obtained in both cycles of the DSC analysis.
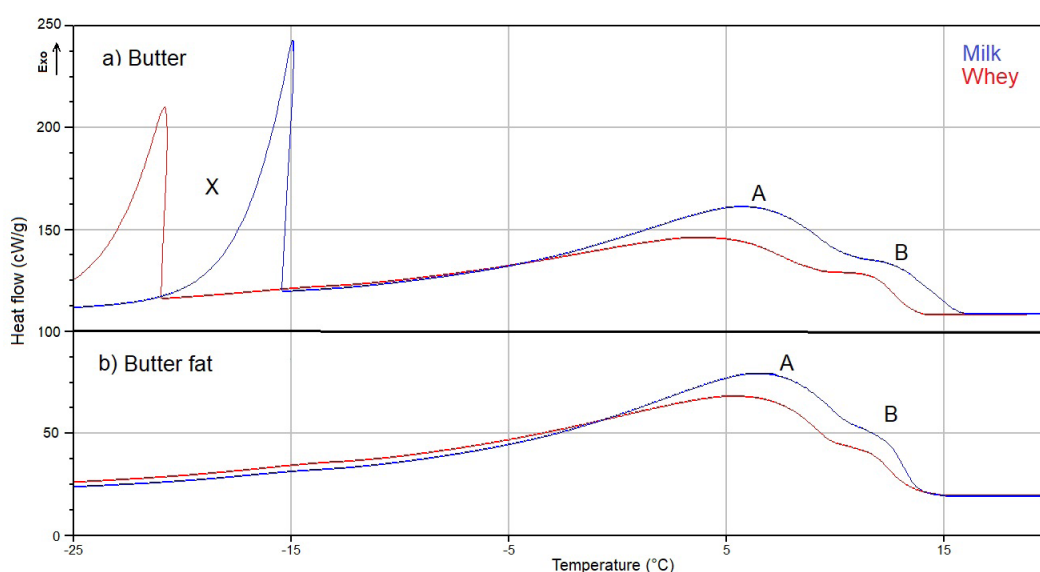

FIGURE 2. Exothermic peaks of fat crystallisation (A, B) and water freezing (X) in milk butter and whey butter (a) and the corresponding fats (b).
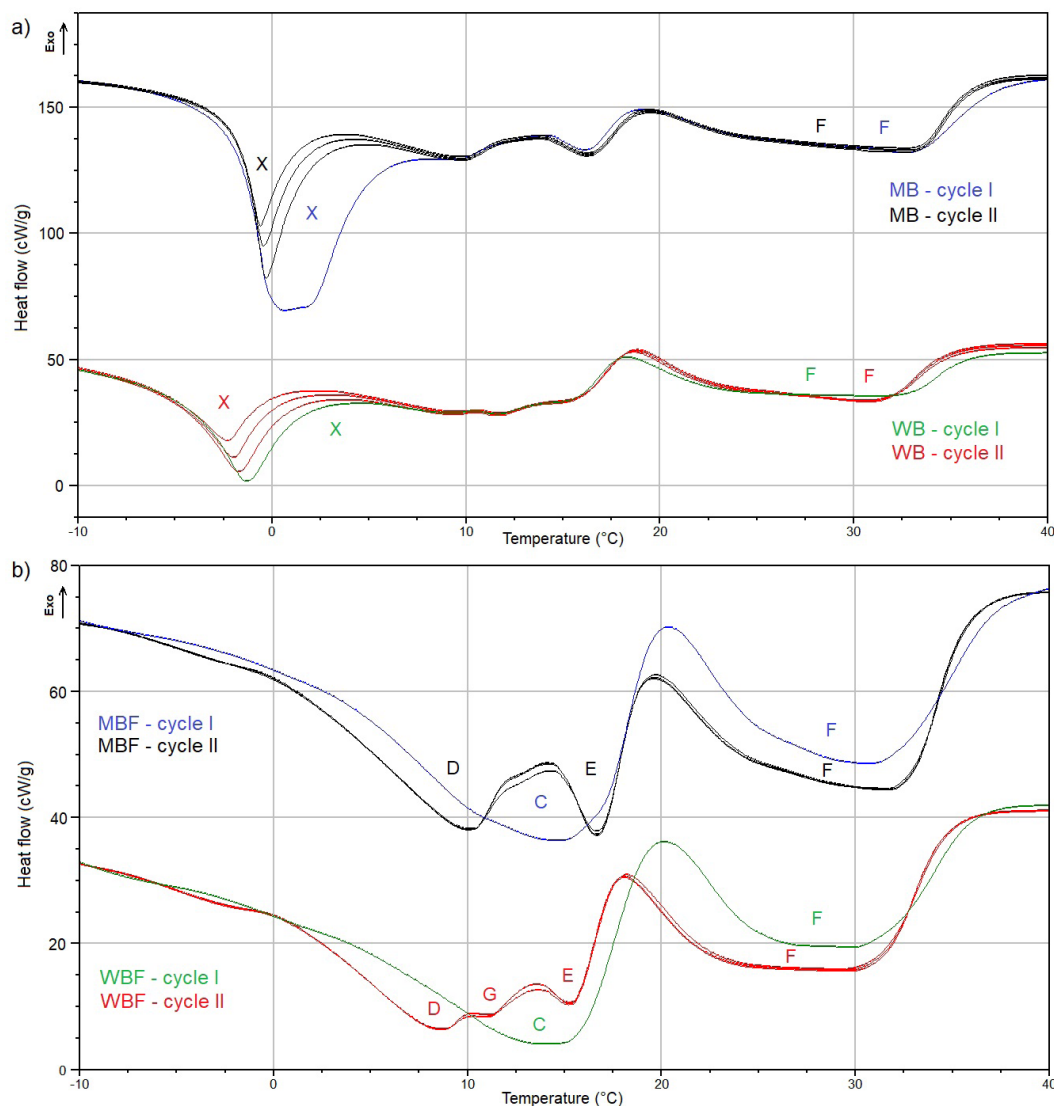
FIGURE 3. Melting curves of milk butter (MB), whey butter (WB) (a) and the corresponding fats (MBF and WBF, respectively) (b) in cycle I and cycle II of the differential scanning calorimetry (DSC) analysis. Endothermic peaks represent: C – low-melting point fraction (LMPF) and middle--melting point fraction (MMPF) melting; D and G – LMPF melting; E – MMPF melting; F – high-melting point fraction (HMPF) melting. Peaks X denote ice melting (a).

Peak B was not completely separated from peak A at a cooling rate of 10°C/min, therefore peaks A and B were determined jointly as a single exothermic peak (undifferentiated peaks A and B) (Table 2). Exothermic peaks (Figure 2) had similar characteristics to those reported by Smet *et al.* [2010]. In a mentioned study, onset temperature was determined at 15.35°C in the first crystallisation peak and at 12.07°C in the second crystallisation peak. Exothermic peaks (A–B) were associated with crystallisation that occurs within a temperature range of –40°C to 20°C [Brożek *et al.*, 2022a, b; Hokkanen *et al.*, 2021; Smet *et al.*, 2010]. Truong *et al.* [2014] noted two peaks between 0°C to 15°C in hard milk fat fraction. A first peak within the temperature range of 0°C to 10°C and a second additional smaller peak between 10°C to 15°C.

An analysis of the exothermic peaks of milk fat crystallisation demonstrated that water removal had no significant (p>0.05) effect on T_{max} values in MB samples or T_{max} and T_{onset} values in WB samples (Table 2). The remaining parameters

of the exothermic peaks of fat crystallisation differed significantly ($p \leq 0.05$) between MB and MBF as well as between WB and WBF. T_{onset} was the only parameter that did not differ significantly ($p > 0.05$) between MBF and WBF. Values of parameters ΔH and P_{height} were higher in the crystallisation peaks of MBF and WBF than in the crystallisation peaks of MB and WB, respectively, due to a higher content of milk fat.

Endothermic peaks were observed in DSC curves in the range of –40°C to 40°C, especially in the range of –10°C to 40°C, during heating within a temperature range of –40°C to 95°C (Figure 3). The DSC curves presenting fat melting parameters differed across DSC cycles. Two endothermic peaks (C and F) were noted in cycle I, whereas four endothermic peaks (D–G) that did not change in successive heating and cooling treatments were observed in cycle II. The first peak (C) with an unclear onset temperature and its endset at 16–21°C was observed only in cycle I. Peak C was associated with unseparated LMPF and MMPF. In cycle II of the DSC

TABLE 2. Parameters of exothermic phase transition peaks – undifferentiated peaks A and B in cycle II of the differential scanning calorimetry (DSC) analysis of milk butter (MB), milk butter fat (MBF), whey butter (WB) and whey butter fat (WBF).

Sample	T_{max} (°C)	T_{onset} (°C)	ΔH (J/g)	$\Delta T_{1/2}$ (°C)	P_{height} (cW/g)	P_s (°C)	P_e (°C)
MB	6.10±0.05[a]	15.75±0.12[a]	42.49±0.92[c]	13.42±0.08[c]	47.82±0.28[b]	16.24±0.19[a]	*
MBF	6.03±0.04[a]	14.02±0.14[b]	64.31±0.27[a]	15.33±0.18[b]	59.04±0.08[a]	15.68±0.05[b]	−37.55±0.49[a]
WB	4.93±0.04[b]	13.89±0.06[b]	36.11±0.17[d]	15.53±0.19[b]	36.87±0.07[c]	14.74±0.21[c]	*
WBF	5.05±0.03[b]	13.70±0.21[b]	59.17±0.29[b]	17.54±0.05[a]	48.38±0.30[b]	14.12±0.10[d]	−38.53±0.18[b]

The values are means ± standard deviations (n=3); values with different superscripts (a–d) in column differ significantly at $p \leq 0.05$. T_{max} – maximum peak temperature; T_{onset} – phase transition onset temperature; ΔH – enthalpy; $\Delta T_{1/2}$ – transition temperature range as peak width at half height; P_{height} – peak height at maximum; P_s – starting point of the peak; P_e – ending point of the peak.

*No clear endset temperature (the water crystallisation peak was not considered in the identification of the end of peak A).

analysis, peak C was transformed to peaks D and E. Peak D was identified as LMPF; it did not have a clear onset temperature, and its endset temperature was determined at 13–15°C. Peak G that was not clearly separated from peak D was observed only on WBF curves within a temperature range of 10–13°C. Peaks G and D represented LMPF melting; therefore, they were considered jointly as a single peak D during the determination of endothermic phase transition peaks (Table 3). Peak E (from 13–14°C to 18–19°C) was identified as MMPF and peak F (from 18–24°C to 34–42°C) was identified as HMPF. Endothermic peaks (C–F) were identified as overlapping LMPF and MMPF peaks (C), and as separate LMPF (D and G), MMPF (E), and HMPF peaks (F) based on published data [Brożek et al., 2022a; Hokkanen et al., 2021; Kasapcopur et al., 2021; Smet et al., 2010; Staniewski et al., 2021]. Our previous study demonstrated that the characteristics of the crystallisation and melting peaks of fat from freeze-dried milk, cream and buttermilk were affected by the content of fat and FAs in samples [Brożek et al., 2022a]. Two fat crystallisation peaks in the DSC curves of buttermilk and milk, and three crystallisation peaks in the DSC curve of cream were reported due to a higher concentration of SFAs in cream than in buttermilk and milk. Małkowska et al. [2021] also observed three crystallisation peaks of the solid fraction of milk fat with a high content of SFAs.

The presence of water in MB and WB had a greater influence on the parameters describing the melting peaks of LMPF and MMPF than HMPF (Table 3) due to the presence of ice melting peaks overlapping LMPF and MMPF melting peaks in DSC curves (Figure 3). Ice melting peaks overlapped milk fat melting peaks C–E in the DSC curves of MB and WB; therefore, the corresponding parameters could not be determined. For this reason, only the parameters of endothermic peaks denoting HMPF melting (peak F) could be compared between cycle I and cycle II. The identification of peaks D and E in DSC curves depended on the size of the ice melting peak. Due to the higher water content in WB than in MB, ice melting peaks were larger on the DSC curve of WB, and they showed greater overlap with peaks C–E than on the DSC curve of MB (Figure 1). Tomaszewska-Gras [2012] found that ΔH of the ice melting peak and the water freezing peak were dependent on the water content of butter.

The parameters of endothermic peaks (C–F) (Figure 3) are presented in Table 3. A comparison of all products and

products within each group (MB and MBF; WB and WBF) revealed that the parameters of the endothermic peaks (C–F) of butters and the corresponding fats differed significantly ($p \leq 0.05$) in most cases. In cycle I of the DSC analysis, the P_{height} of peak C differed between MBF and WBF ($p \leq 0.05$). In peak C, lower values of P_{height} indicate that the phase transition of MBF components was a less energy-intensive process than the phase transition of WBF components. In cycle I of the DSC analysis, the parameters describing peak F differed significantly ($p \leq 0.05$) across products (excluding P_e). In cycle I, differences ($p \leq 0.05$) in T_{onset} and P_s values were noted between MB and MBF and between WB and WBF, whereas no differences ($p > 0.05$) in the values of P_e were observed between MB and WB, or in the values of P_s and P_e between MBF and WBF. The above indicates that fat type did not determine the beginning and end of HMPF melting in cycle I, unlike water which influenced the beginning of HMPF melting in cycle I.

In cycle II, peak C was transformed to LMPF (D) and MMPF peaks (E) (Figure 3). A comparison of MBF and WBF did not reveal significant ($p > 0.05$) differences in the T_{onset} and P_s values of peak D (Table 3), which indicates that the type of butter fat had no effect on the onset of LMPF melting. In turn, MBF and WBF differed significantly ($p \leq 0.05$) in all parameters of peak E, which indicates that the type of butter fat determined the melting characteristics of MMPF. In cycle II of the DSC analysis, the parameters describing peak F differed ($p \leq 0.05$) between MBF and WBF (except for $\Delta T_{1/2}$ and P_e). The differences ($p > 0.05$) were found between MB and MBF (T_{max}, T_{onset} and P_s) and between WB and WBF (T_{max} and T_{onset}), which indicates that water content influenced the mentioned parameters of the HMPF peak in cycle II.

The thermal history of butters and the corresponding fats affected DSC curves showing their melting behaviour (Figure 3) and the parameters of endothermic peaks (Table 3). The greatest differences were noted between LMPF and MMPF. After the first stage of heating, cooling and reheating, the overlapping melting peaks of LMPF and MMPF (peak C) split into separate LMPF (peak D) and MMPF (peak E) peaks. Peak C was completely transformed to peak D (peaks D and G in WBF) and peak E; therefore, the corresponding parameters could not be accurately compared between cycle I and cycle II, and only a general change trend was confirmed. The applied thermal processing regime also influenced HMPF melting parameters (peak F). The endothermic peaks of MBF

414

Pol. J. Food Nutr. Sci., 2022, 72(4), 407–419

TABLE 3. Parameters of endothermic phase transition peaks in cycle I and cycle II of the differential scanning calorimetry (DSC) analysis of milk butter (MB), milk butter fat (MBF), whey butter (WB) and whey butter fat (WBF).

Peak	Cycle	Sample	T_{max} (°C)	T_{onset} (°C)	ΔH (J/g)	$\Delta T_{1/2}$ (°C)	P_{height} (cW/g)	P_s (°C)	P_e (°C)
C	I	MB	n.d.	n.d.	n.d.	n.d.	n.d.	n.d.	n.d.
		MBF	15.25±0.58[a]	2.88±1.16[a]	19.66±1.63[a]	10.97±0.57[a]	−31.01±1.15[b]	*	20.68±0.51[a]
		WB	n.d.	n.d.	n.d.	n.d.	n.d.	n.d.	n.d.
		WBF	15.05±0.65[a]	2.43±2.37[a]	15.91±2.40[a]	10.27±1.34[a]	−27.48±1.52[a]	*	20.14±0.14[a]
D	II	MB	n.d.	n.d.	n.d.	n.d.	n.d.	n.d.	n.d.
		MBF	9.41±0.08[a]	1.48±0.33[a]	5.51±0.49[a]	6.33±0.21[b]	−12.22±0.71[b]	0.12±0.41[a]	14.42±0.10[a]
		WB	n.d.	n.d.	n.d.	n.d.	n.d.	n.d.	n.d.
		WBF	7.90±0.28[b]	1.36±0.34[a]	4.12±0.68[b]	7.71±0.25[a]	−9.93±1.58[a]	0.02±0.32[a]	13.82±0.36[b]
E	II	MB	n.d.	n.d.	n.d.	n.d.	n.d.	n.d.	n.d.
		MBF	17.17±0.03[a]	14.98±0.08[a]	2.22±0.14[a]	2.43±0.13[a]	−16.13±0.90[b]	14.47±0.11[a]	19.90±0.07[a]
		WB	n.d.	n.d.	n.d.	n.d.	n.d.	n.d.	n.d.
		WBF	16.22±0.04[b]	14.26±0.05[b]	0.81±0.19[b]	2.07±0.16[b]	−7.02±0.85[a]	13.91±0.06[b]	18.46±0.04[b]
F	I	MB	32.46±0.51[aA]	19.71±0.47[cA]	15.62±1.04[aA]	11.32±0.45[bA]	−25.26±1.61[bA]	19.18±0.13[bA]	41.84±2.32[aA]
		MBF	31.64±0.61[aA]	21.66±0.32[aA]	15.76±0.82[aA]	10.85±0.40[cA]	−25.59±1.37[bA]	21.11±0.81[aA]	41.99±0.91[aA]
		WB	30.21±0.80[bA]	18.72±0.09[dA]	12.52±0.91[bA]	11.81±0.65[aA]	−19.54±1.86[aA]	18.25±0.08[cA]	39.78±1.95[aA]
		WBF	30.33±0.37[bA]	20.90±0.32[bA]	12.68±0.79[bA]	11.76±0.42[aA]	−19.73±1.59[aA]	20.43±0.52[aA]	39.97±1.07[aA]
	II	MB	32.67±0.33[aA]	19.96±0.26[bA]	15.19±0.72[aA]	11.52±0.21[aA]	−26.48±0.69[bA]	19.48±0.26[bA]	41.25±0.91[aA]
		MBF	32.04±0.21[bA]	20.46±0.13[aB]	15.56±0.37[aA]	11.40±0.19[aA]	−25.79±0.41[bA]	19.95±0.17[aB]	39.96±0.50[abB]
		WB	31.05±0.35[bA]	18.78±0.31[cA]	13.36±0.62[bA]	12.09±0.30[aA]	−21.95±1.18[aA]	18.35±0.24[cA]	38.50±1.29[bA]
		WBF	30.49±0.24[cA]	19.30±0.20[bB]	13.57±0.26[bA]	11.63±0.15[aA]	−21.35±0.47[aA]	18.53±0.11[cB]	40.11±0.17[abA]

The values are means ± standard deviations ($n=3$); values with different lowercase letters (a–d) in superscripts in column separately for each peak and cycle differ significantly at $p \le 0.05$; values with different uppercase letters (A–B) in superscripts for individual product in cycle I and cycle II of peak F differ significantly at $p \le 0.05$. T_{max} – maximum peak temperature; T_{onset} – phase transition onset temperature; ΔH – enthalpy; $\Delta T_{1/2}$ – transition temperature range as peak width at half height; P_{height} – peak height at maximum; P_s – starting point of the peak; P_e – ending point of the peak; n.d. – not detected (the water freezing peak overlapped fat melting peaks).

and WBF differed in T_{onset} and P_s values, and the endothermic peak of MBF differed ($p \le 0.05$) in the value of P_e between cycle I and cycle II (Table 3). In the DSC analysis, the peak parameters of all products were less scattered in cycle II than in cycle I, which indicates that the milk fat melting process was more stable in cycle II. The transition of peak C to peaks D and E (Figure 3) and the smaller scatter of results in cycle II than in cycle I (Table 3) could be explained by the transition of fat crystals from the polymorphic form α to forms β' and β. According to the literature, the hexagonal α form is irreversibly transformed to the more stable orthorhombic β' and triclinic β forms during thermal processing [Fredrick *et al.*, 2011; Hondoh & Ueno, 2016; Lopez & Ollivon, 2009; Staniewski *et al.*, 2021; Viriato *et al.*, 2019]. Our previous study demonstrated that thermal history influenced the parameters of phase transition peaks and fat melting peaks of cream, milk, and buttermilk [Brożek *et al.*, 2022b]. In turn, Staniewski *et al.* [2020] found that thermal history affected the melting process of anhydrous milk fat.

The following variables were subjected to PCA to identify variables that were most highly correlated with MBF and WBF, as well as variables that were bound by the strongest correlations: the FA profile of samples (g/100 g total FAs) (Table 1) and the peak parameters (Table 2 and Table 3). The first two principal components, PC1 and PC2, explained 80.50% of total variance in input data, but only PC1 explained 69.78% of the variance, whereas PC2 explained only 10.72% of the variance (Figure 4). Two clusters of variables (left and right) were formed at the ends of the PC1 axis. The variables from each cluster were strongly correlated with each other.

The loading vectors indicate that the variables were correlated. The greater the acute angle, the stronger the correlation between the variables in a given direction, whereas an obtuse angle points to an inverse correlation, and a straight angle indicates an absence of a correlation between variables. To facilitate the description of variables, peaks were marked with letters A and C–F, and the symbols I and II in the subscript denote cycles I and II, respectively. The cluster on the left side of the PC plot contains points representing variables with negative loadings on the PC1 axis in the range of –0.99 to –0.75 (Figure 4). These variables were higher in WBF than
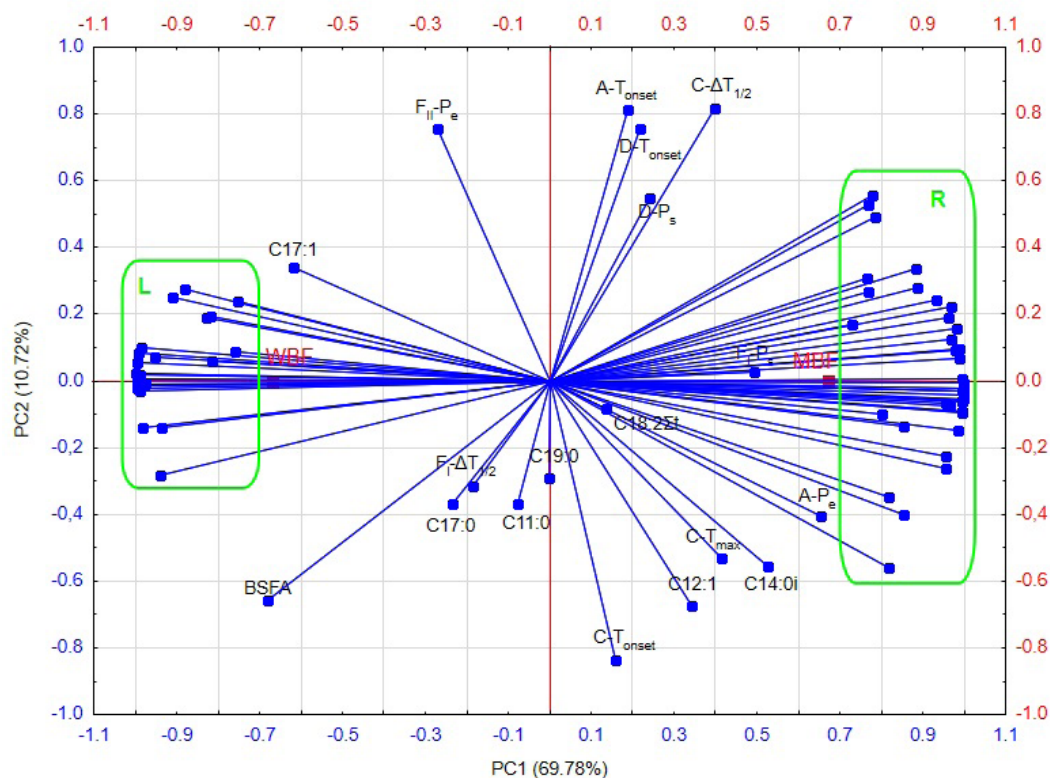
FIGURE 4. Principal component analysis biplot of milk butter fat (MBF) and whey butter fat (WBF), and the contribution of the parameters of peaks C and F in cycle I and peaks A, D, E and F in cycle II of the differential scanning calorimetry (DSC), and the content fatty acids (g/100 g total fatty acids) to principal component 1 (PC1) and principal component 2 (PC2). The variables were arranged in ascending (cluster left, L) and descending (cluster right, R) order based on loadings. The L cluster contains C15:0 *ai*, C18:1 Σt, D-$\Delta T_{1/2}$, F_{II}-P_{height}, C18:3, C18:2 *c*9, *t*11, C15:0 *i*, MUFA, PUFA, C18:2, C18:1 Σc, LCFA, E-P_{height}, A-$\Delta T_{1/2}$, C18:0, F_I-P_{height}, C-P_{height}, C4:0, SCFA, C8:0, D-P_{height}, C6:0, F_{II}-$\Delta T_{1/2}$. The R cluster contains C16:0, C14:1, C16:1, C14:0, F_{II}-T_{max}, C12:0, C13:0 *ai*, C13:0, SFA, MCFA, A-P_{height}, F_{II}-P_s, F_{II}-ΔH, C10:0, F_{II}-T_{onset}, C10:1, A-ΔH, D-T_{max}, C15:0, E-P_e, E-ΔH, F_I-ΔH, A-P_s, E-T_{max}, F_I-T_{max}, E-T_{onset}, A-T_{max}, C13:0 *i*, E-$\Delta T_{1/2}$, C16:0 *i*, D-ΔH, E-P_s, D-P_e, C-P_e, C-ΔH, F_I-P_e and F_I-T_{onset}. Symbols I, II in the subscript of peak F denote cycles I and II of the DSC analytical sequence, respectively.

in MBF. The left cluster includes the following variables: C15:0 *ai*, C18:1 Σt, D-$\Delta T_{1/2}$, F_{II}-P_{height}, C18:3, C18:2 *c*9, *t*11, C15:0 *i*, MUFA, PUFA, C18:2, C18:1 Σc, LCFA, E-P_{height}, A-$\Delta T_{1/2}$, C18:0, F_I-P_{height}, C-P_{height}, C4:0, SCFA, C8:0, D-P_{height}, C6:0, and F_{II}-$\Delta T_{1/2}$, which were arranged in an ascending order based on the loadings. The cluster on the right side of the PC1 axis contains points denoting variables that were bound by inverse correlations relative to the left cluster and were characterised by highly positive loadings in the range of 0.73 to 0.99. The values of these variables were higher in MBF than in WBF. The right cluster includes following variables: C16:0, C14:1, C16:1, C14:0, F_{II}-T_{max}, C12:0, C13:0 *ai*, C13:0, SFA, MCFA, A-P_{height}, F_{II}-P_s, F_{II}-ΔH, C10:0, F_{II}-T_{onset}, C10:1, A-ΔH, D-T_{max}, C15:0, E-P_e, E-ΔH, F_I-ΔH, A-P_s, E-T_{max}, F_I-T_{max}, E-T_{onset}, A-T_{max}, C13:0 *i*, E-$\Delta T_{1/2}$, C16:0 *i*, D-ΔH, E-P_s, D-P_e, C-P_e, C-ΔH, F_I-P_e, and F_I-T_{onset}, which were arranged in a descending order based on the loadings.

A higher content of SFAs and MCFAs, especially C12:0, C14:0 and C16:0, in MBF than in WBF increased the values of T_{max}, ΔH and P_s and decreased the value of $\Delta T_{1/2}$ in crystallisation peak A (which indicates that MBF crystallisation was characterised by higher enthalpy, occurred at a higher temperature, and proceeded less rapidly than WBF crystallisation), whereas an increase in the content of MUFAs, PUFAs, and LCFAs, including C18:1, and, to a much

lesser degree, an increase in the content of SCFAs, including C4:0, C6:0 and C8:0, induced a reverse trend (which indicates that WBF crystallisation was characterised by lower enthalpy, occurred at a lower temperature, and proceeded more rapidly than MBF crystallisation). In our previous study, we found that T_{onset} increased, whereas $\Delta T_{1/2}$ decreased with a rise in the content of SFAs and MCFAs, in particular C14:0 and C16:0, in freeze-dried milk [Brożek *et al.*, 2022b]. In turn, Truong *et al.* [2014] reported that anhydrous milk fat had a crystallisation peak in the temperature range from –5°C to 10°C. The observed peak was smaller and characterised by higher values of T_{max} and T_{onset} in the hard fraction compared to soft fraction of milk fat.

The content of SFAs and MCFAs, especially C12:0, C14:0 and C16:0, influenced the value of P_e of the melting peak corresponding to the merged LMPF and MMPF peaks (peak C); the values of T_{max}, ΔH and P_e of the LMPF peak (peak D); the values of T_{max}, T_{onset}, ΔH, $\Delta T_{1/2}$, P_s and P_e of the MMPF peak (peak E); the values of T_{max}, T_{onset}, ΔH and P_e in cycle I; and the values of T_{max}, T_{onset}, ΔH and P_s in cycle II of the HMPF melting peak (peak F). The above implies that the maximum difference in heat flow in all endothermic peaks (based on the absolute values in cycles I and II), the enthalpy of LMPF, MMPF and HMPF (in cycles I and II), and the melting rate of MMPF were lower in WBF than MBF, whereas the beginning

416

Pol. J. Food Nutr. Sci., 2022, 72(4), 407–419

TABLE 4. Colour parameters of milk butter (MB) and whey butter (WB).

Sample	L^*	a^*	b^*	C^*	WI	YI	ΔC^*	ΔE
MB	89.13±0.43[a]	−3.41±0.03[a]	32.08±0.11[a]	32.26±0.11[a]	65.96±0.15[b]	51.42±0.25[a]	2.25±0.11	2.33±0.27
WB	88.96±0.58[a]	−3.17±0.06[b]	29.84±0.23[b]	30.01±0.23[b]	68.02±0.02[a]	47.92±0.05[b]		

Values are means ± standard deviations ($n=3$); values with different superscripts in column differ significant at $p\leq0.05$. L^* – lightness; a^* – position between redness and greenness; b* – position between blueness and yellowness; C^* – chromaticity; WI – whiteness index; YI – yellowness index; ΔE – total colour difference; ΔC^* – difference in saturation.

of MMPF (peak E) and HMPF (cycles I and II, peak F) melting and the end of melting in the overlapping peaks of LMPF and MMPF (peak C), LMPF (peak D) and MMPF (peak E) occurred at a lower temperature in WBF than MBF. The content of MUFAs, PUFAs, and LCFAs, including C18:0, and to a much smaller extent, the content of SCFAs, including C4:0, C6:0 and C8:0, induced a drop in the above parameters, but increased P_{height} values of all endothermic peaks, and $\Delta T_{1/2}$ values of LMPF and HMPF (cycle II) melting peaks. The above implies that LMPF and HMPF (cycle II) melted more rapidly in WBF than MBF. The presence of peak G can probably be attributed to a higher content of MUFAs, PUFAs, and LCFAs, including C18:0, in WBF than in MBF. According to Staniewski *et al.* [2021], the FA profile of TAGs can affect the melting behaviour of milk fat, in particular the value of P_s, and it can influence the textural properties of butter. Anankanblil *et al.* [2018] demonstrated that the P_s value of MMPF and HMPF crystallisation and melting peaks decreased with a rise in the content of C18:0, C18:1, C18:2, and C18:3, and increased with a rise in the content of C14:0 and C16:0. Larsen *et al*. [2014] and Smet *et al*. [2010] made similar observations also in the P_s value of the LMPF peak. The saturated FA C18:0 decreased the P_s values of milk fat crystallisation and melting peaks despite the fact that it has a higher melting temperature than C18:1, C18:2, and C18:3. The above could be attributed to mammary desaturase activity which transforms C18:0 into C18:1, thus lowering melting temperature [Anankanblil *et al.*, 2018; Larsen *et al.*, 2014]. Buldo *et al.* [2013] reported a correlation between the melting temperature (P_s) of MMPF and the content of C14:1, C16:0, C18:1 Σc, C18:1 Σt, and C18:2 $c9$, $t11$. In a PCA conducted in our previous study, the content of many FAs was correlated with the parameters of crystallisation and melting peaks of fat from freeze-dried milk, including the values of T_{onset} of the crystallisation peak, $\Delta T_{1/2}$ of the LMPF melting peak, and T_{max} and T_{onset} of the MMPF peak [Brożek *et al.,* 2022b]. These variables were inversely corelated with the $\Delta T_{1/2}$ of the crystallisation peak and the content of LCFAs, MUFAs, and PUFAs, including C18:0, C18:1, C18:2 and C18:3.

TABLE 5. Textural properties of milk butter (MB) and whey butter (WB).

Sample	Firmness (N)	Consistency (N×s)	Cohesiveness (N)	Viscosity (N×s)
MB	1.80±0.05[a]	30.90±0.74[a]	−0.86±0.07[b]	−1.54±0.19[a]
WB	1.68±0.06[b]	30.67±1.59[a]	−0.67±0.08[a]	−1.30±0.03[a]

Values are means ± standard deviation ($n=3$); values with different superscripts in column differ significantly at $p\leq0.05$.

Colour

Samples of MB and WB differed significantly ($p\leq0.05$) in the colour parameters a^*, b^*, C^*, WI and YI, but not in parameter L^* ($p>0.05$) (Table 4). The values of b^* and YI were higher in MB, which indicates that it was more yellow in colour than WB. Colour chroma was also higher in MB, whereas the values of parameter a^* and the whiteness index were higher in WB.

The values of L^*, a^* and b^* in MB were similar to those given in the literature [Gómez-Mascaraque *et al.*, 2020]. In turn, WB was characterised by similar lightness, a higher contribution of greenness, and a significantly higher contribution of yellowness relative to other studies [Jinjarak *et al.*, 2006; Kasapcopur *et al.*, 2021]. The total colour difference between MB and WB reached 2.33 (Table 4). The detection of colour difference could be easily possible even by an inexperienced observer if the $\Delta E=2.0–3.5$ [Dobrzańska & Cais-Sokolińska, 2014].

Texture

The textural properties of MB and WB are presented in Table 5. Milk butter and whey butter differed significantly ($p\leq0.05$) in firmness. Internal stickiness (described by cohesiveness values) was significantly ($p\leq0.05$) higher in MB than WB. The examined products did not differ significantly ($p>0.05$) in consistency or viscosity. The obtained lower values of firmness and cohesiveness for WB compared to MB are in agreement with the fatty acid profiles of the samples. In turn WB was more abundant in MUFAs and PUFAs (Table 1) which contribute to butter softness. Amal [2009] and Jinjarak *et al.* [2006] reported lower hardness and cohesiveness in whey butter than in sweet cream butter. In the work of Staniewski *et al.* [2021], the rheological properties of butter were correlated with the composition of TAGs in the fat phase, and butter firmness decreased with a rise in the content of C18:1, C18:2, and C18:3 PUFAs in TAGs.

Sensory evaluation

The sensory evaluation revealed that MB and WB differed significantly ($p\leq0.05$) in the values of consistency descriptors: firmness, brittleness, and cohesiveness (Figure 5) as well as in the intensity of milky and nutty aroma, and cheesy taste ($p\leq0.05$). The remaining descriptors of taste, aroma, and colour uniformity did not differ significantly ($p>0.05$) between the compared butters.

In a study by Mallia *et al.* [2008], butter enriched with UFAs was characterised by higher spreadability and a somewhat less intense milky taste and pasteurisation aroma than
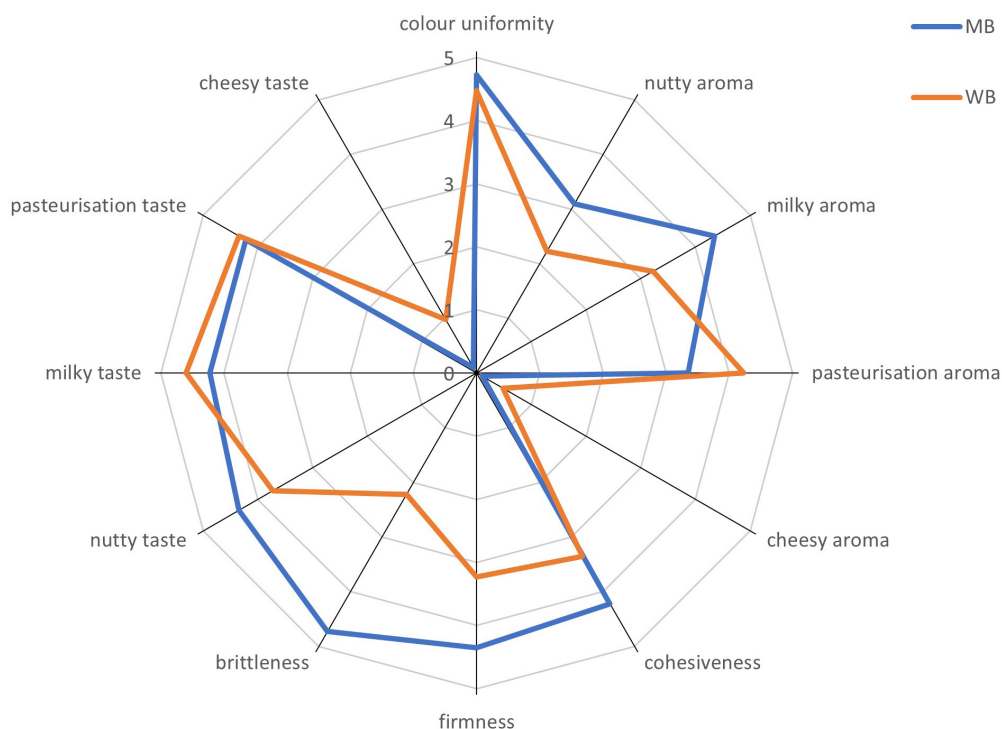
FIGURE 5. Sensory profile of milk butter (MB) and whey butter (WB).

CONCLUSIONS

Whey butter had comparable sensory attributes to MB, but it was less yellow in colour. Whey butter was softer than MB due to a higher content of MUFAs, PUFAs, and LCFAs, leading to lower crystallisation onset temperature and higher melting onset temperature of fat. The thermal properties of butter were determined by butter type, FA profile, presence of water, and thermal history. Due to relatively high water content, the DSC curves of butter differed considerably from the DSC curves of butter fat. Water freezing and ice melting peaks overlapped fat crystallisation and melting peaks, which hindered their observations in DSC curves and affected their parameters. The phase transition peaks of milk fat and water, peak overlaps, and the extent to which water affected the parameters of milk fat phase transition peaks were determined based on an analysis of the DSC curves of butters and their fats. Thermal history influenced butter melting behaviour by inducing changes in DSC curves, including the number of peaks and peak parameters. The PCA revealed that a rise in the content of SFAs and MCFAs, especially C12:0, C14:0 and C16:0; increased the values of T_{max}, ΔH and P_s; decreased the value of $\Delta T_{1/2}$ of the crystallisation peak; increased the value of P_e of the merged melting peak of LMPF and MMPF; increased the values of T_{max}, ΔH and P_e of the LMPF peak; increased the values of T_{max}, T_{onset}, ΔH, $\Delta T_{1/2}$, P_s and P_e of the MMPF peak; increased the values of T_{max}, T_{onset}, ΔH and P_e in cycle I; and increased the values of T_{max}, T_{onset}, ΔH and P_s in cycle I of the HMPF peak. Reverse trends were observed with a rise in the content of MUFAs, PUFAs, and LCFAs, including C18:0, and to a smaller extent, with an increase in the content of SCFAs, in particular C4:0. These results were used to determine the influence of butter type on the crystallisation and melting characteristics of WBF and MBF. WBF crystallisation was characterised by lower enthalpy; it occurred at a lower temperature, and proceeded more rapidly than MBF crystallisation. In turn, LMPF and HMPF (cycle II) melted more rapidly in WBF than MBF, whereas the absolute maximum difference in heat flow in all fractions (cycles I and II), the enthalpy of LMPF, MMPF and HMPF (cycles I and II), the melting rate of MMPF, and the values at the beginning (MMPF and HMPF in cycles I and II) and the end of melting (overlapping LMPF and MMPF peaks in cycle I; separate LMPF and MMPF peaks in cycle II) were lower in WBF than MBF. Whey butter and milk butter differed in physicochemical properties and sensory attributes, and their thermal profiles depended on the FA profile, water content, and thermal history.

conventional butter after 1 week of storage at 6°C. After 8 weeks of storage at 6°C, these differences, excluding spreadability, were levelled out between the samples. Jinjarak *et al.* [2006] found that sweet cream butter and whey butter differed significantly only in yellowness, shininess, porosity, melting rate, cardboard odour, and nutty flavour.

CONFLICT OF INTERESTS

The authors declare that they have no known competing financial interests or personal relationships that could have appeared to influence the work reported in this paper.

ORCID IDs

K. Bohdziewicz https://orcid.org/0000-0003-2394-0495
O.M. Brożek https://orcid.org/0000-0002-0133-3224
K. Kiełczewska https://orcid.org/0000-0002-5267-925X

REFERENCES

1. Amal, A.H. (2009). Fatty acid composition, textural and organoleptic properties of whey butter. *Journal of Food and Dairy Sciences*, *34*(4), 3081–3094.
https://doi.org/10.21608/JFDS.2009.11343

2. Amara-Dali, W.B, Lesieur, P., Artzner, F., Karray, N., Attia, H., Ollivon, M. (2007). Anhydrous goat's milk fat: thermal and structural behaviors studied by coupled differential scanning calorimetry and X-ray diffraction. 2. Influence of cooling rate. *Journal of Agricultural and Food Chemistry*, *55*(12), 4741–4751.
https://doi.org/10.1021/jf063210p

3. Anankanbil, S., Larsen, M.K., Weisbjerg, M.R., Wiking, L. (2018). Effects of variation in fatty acids and triglyceride composition on melting behavior in milk fat. *Milk Science International*, *71*(2), 4–9.
https://doi.org/10.25968/MSI.2018.2

4. Brighenti, M., Govindasamy-Lucey, S., Jaeggi, J.J., Johnson, M.E., Lucey, J.A. (2021). Effect of substituting whey cream for sweet cream on the textural and rheological properties of cream cheese. *Journal of Dairy Science*, *104*(10), 10500–10512.
https://doi.org/10.3168/jds.2021-20338

5. Brożek, O.M., Kiełczewska, K., Bohdziewicz, K. (2022a). Fatty acid profile and thermal characteristics of ovine and bovine milk and their mixtures. *International Dairy Journal*, *129*, art. no. 105339.
https://doi.org/10.1016/j.idairyj.2022.105339

6. Brożek, O.M., Kiełczewska, K., Bohdziewicz, K. (2022b). Characterisation of selected emulsion phase parameters in milk, cream and buttermilk. *Polish Journal of Food and Nutrition Sciences*, *72*(1), 5–15.
https://doi.org/10.31883/pjfns/144223

7. Buldo, P., Larsen, M.K., Wiking, L. (2013). Multivariate data analysis for finding the relevant fatty acids contributing to the melting fractions of cream. *Journal of the Science of Food and Agriculture*, *93*(7), 1620–1625.
https://doi.org/10.1002/jsfa.5934

8. Çetinkaya, A. (2021). A research on determination of some properties of butter made from creams extracted from whey and milk. *European Journal of Agriculture and Food Sciences*, *3*(4), 19–24.
https://doi.org/10.24018/ejfood.2021.3.4.321

9. Couvreur, S., Hurtaud, C., Lopez, C., Delaby, L., Peyraud, J.L. (2006). The linear relationship between the proportion of fresh grass in the cow diet, milk fatty acid composition, and butter properties. *Journal of Dairy Science*, *89*(6), 1956–1969.
https://doi.org/10.3168/jds.S0022-0302(06)72263-9

10. Dobrzańska, A., Cais-Sokolińska, D. (2014). Measuring the brightness and coordinate trichromaticity milk protein preparations. *Aparatura Badawcza i Dydaktyczna*, *19*(3), 267–272 (in Polish; English abstract).

11. Fauquant, C., Briard, V., Leconte, N., Michalski, M.-C. (2005). Differently sized native milk fat globules separated by microfiltration: fatty acid composition of the milk fat globule membrane and triglyceride core. *European Journal of Lipid Science and Technology*, *107*(2), 80–86.
https://doi.org/10.1002/ejlt.200401063

12. Food and Agriculture Organization/World Health Organization. (2018). *Codex Alimentarius: Standard for butter, CXS 279-1971. Amended in 2018.* Food and Agriculture Organisation of the United Nations, Rome, Italy.

13. Fredrick, E., Van de Walle, D., Walstra, P., Zijtveld, J.H., Fischer, S., Van der Meeren, P., Dewettinck, K. (2011). Isothermal crystallization behaviour of milk fat in bulk and emulsified state. *International Dairy Journal*, *21*(9), 685–695.
https://doi.org/10.1016/j.idairyj.2010.11.007

14. Gómez-Mascaraque, L.G., Kilcawley, K., Hennessy, D., Tobin, J.T., O'Callaghan, T.F. (2020). Raman spectroscopy: A rapid method to assess the effects of pasture feeding on the nutritional quality of butter. *Journal of Dairy Science*, *103*(10), 8721–8731.
https://doi.org/10.3168/jds.2020-18716

15. Hokkanen, S.P., Partanen, R., Jukkola, A., Frey, A.D., Rojas, O.J. (2021). Partitioning of the milk fat globule membrane between buttermilk and butter serum is determined by the thermal behaviour of the fat globules. *International Dairy Journal*, *112*, art. no. 104863.
https://doi.org/10.1016/j.idairyj.2020.104863

16. Hondoh, H., Ueno, S. (2016). Polymorphism of edible fat crystals. *Progress in Crystal Growth and Characterization of Materials*, *62*(2), 398–399.
https://doi.org/10.1016/j.pcrysgrow.2016.04.021

17. International Organization for Standardization. (2002). *Milk fat – Preparation of fatty acid methyl esters* (ISO Standard No. 15884).

18. International Organization for Standardization. (2010). *Milk – Determination of fat content – Gravimetric method (Reference method)* (ISO Standard No. 1211).

19. International Organization for Standardization. (2014). *Sensory analysis. General guidelines for the selection, training and monitoring of selected assessors and expert sensory assessors* (ISO Standard No. 8586).

20. International Organization for Standardization. (2016). *Sensory analysis – Methodology – General guidance for establishing a sensory profile* (ISO Standard No. 13299).

21. Jhanwar, A., Ward, R.E. (2014). Particle size distribution and lipid composition of skim milk lipid material. *International Dairy Journal*, *36*(2), 110–117.
https://doi.org/10.1016/j.idairyj.2014.01.010

22. Jinjarak, S., Olabi, A., Jiménez-Flores, R., Walker, J.H. (2006). Sensory, functional, and analytical comparisons of whey butter with other butters. *Journal of Dairy Science*, *89*(7), 2428–2440.
https://doi.org/10.3168/jds.S0022-0302(06)72316-5

23. Jukkola, A., Rojas, O.J. (2017). Milk fat globules and associated membranes: Colloidal properties and processing effects. *Advances in Colloid and Interface Science*, *245*, 92–101.
https://doi.org/10.1016/j.cis.2017.04.010

24. Kasapcopur, E., Mohammed, A.M., Colakoglu, A.S. (2021). Effects of differences in whey composition on the physicochemical properties of whey butter. *International Journal of Dairy Technology*, *74*(3), 535–546.
https://doi.org/10.1111/1471-0307.12782

25. Larsen, M.K., Andersen, K.K., Kaufmann, N., Wiking, L. (2014). Seasonal variation in the composition and melting behavior of milk fat. *Journal of Dairy Science*, *97*(8), 4703–4712.
https://doi.org/10.3168/jds.2013-7858

26. Lopez, C., Lesieur, P., Bourgaux, C., Ollivon, M. (2005). Thermal and structural behavior of anhydrous milk fat. 3. Influence of cooling rate. *Journal of Dairy Science*, *88*(2), 511–526.
https://doi.org/10.3168/jds.S0022-0302(05)72713-2

27. Lopez, C., Ollivon, M. (2009). Triglycerides obtained by dry fractionation of milk fat: 2. Thermal properties and polymorphic evolutions on heating. *Chemistry and Physics of Lipids*, *159*(1), 1–12.
https://doi.org/10.1016/j.chemphyslip.2009.02.009

28. Macwan, S.R., Dabhi, B.K, Parmar, S.C., Aparnathi, K.D. (2016). Whey and its utilization. *International Journal of Current Microbiology and Applied Sciences*, *5*(8), 134–155.
http://dx.doi.org/10.20546/ijcmas.2016.508.016

29. Mallia, S., Escher, F., Schlichtherle-Cerny, H. (2008). Aroma-active compounds of butter: a review. *European Food Research and Technology*, *226*, 315–325.
https://doi.org/10.1007/s00217-006-0555-y

30. Małkowska, M., Staniewski, B., Ziajka, J. (2021). Analyses of milk fat crystallization and milk fat fractions. *International Journal of Food Properties*, *24*(1), 325–336.
https://doi.org/10.1080/10942912.2021.1878217

31. Michalski, M.-C., Ollivon, M., Briard, V., Leconte, N., Lopez, C. (2004). Native fat globules of different sizes selected from raw milk: thermal and structural behavior. *Chemistry and Physics of Lipids*, *132*(2), 247–261.
https://doi.org/10.1016/j.chemphyslip.2004.08.007

32. Nadeem, M., Mahud, A., Imran, M., Khalique, A. (2014). Enhancement of the oxidative stability of whey butter through almond (*Prunus dulcis*) peel extract. *Journal of Food Processing and Preservation*, *39*(6), 591–598.
https://doi.org/10.1111/jfpp.12265

33. Nishanthi, M., Vasiljevic, T., Chandrapala, J. (2017). Properties of whey proteins obtained from different whey streams. *International Dairy Journal*, *66*, 76–83.
https://doi.org/10.1016/j.idairyj.2016.11.009

34. Omar, K.A., Gounga, M.E., Liu, R., Mwinyi, W., Aboshora, W., Ramadhan, A.H., Sheha, K.A., Wang, X. (2017). Triacylglycerol composition, melting and crystallization profiles of lipase catalysed anhydrous milk fats hydrolysed. *International Journal of Food Properties*, *20*(sup2), 1230–1245.
https://doi.org/10.1080/10942912.2017.1301954

35. Panghal, A., Patidar, R., Jaglan, S., Chhikara, N., Khatkar, S.K., Gat, Y., Sindhu, N. (2018). Whey valorization: current options

and future scenario – a critical review. *Nutrition and Food Science*, *48*(3), 520–535.
https://doi.org/10.1108/nfs-01-2018-0017

36. Pathare, P.B., Opara, U.L., Al-Said, F.A.-J. (2013). Colour measurement and analysis in fresh and processed foods: A review. *Food and Bioprocess Technology*, *6*(1), 36–60.
https://doi.org/10.1007/s11947-012-0867-9

37. Sánchez, L., Pérez, M.D. (2012). Physical properties of dairy products. In I. Arana (Ed.), *Physical Properties of Foods: Novel Measurement Techniques and Applications*, CRC Press, Boca Raton, USA, pp. 355–398.
https://doi.org/10.1201/b11542

38. Smet, K., Coudijzer, K., Fredrick, E., De Campeneere, S., De Block, J., Wouters, J, Raes, K., Dewettinck, K. (2010). Crystallization behavior of milk fat obtained from linseed-fed cows. *Journal of Dairy Science*, *93*(2), 495–505.
https://doi.org/10.3168/jds.2009-2588

39. Staniewski, B., Smoczyński, M., Żulewska, J., Wiśniewska, K., Baranowska, M. (2020). Effect of model heat treatment conditions on selected properties of milk fat. *International Journal of Dairy Technology*, *73*(3), 532–541.
https://doi.org/10.1111/1471-0307.12697

40. Staniewski, B., Ogrodowska, D., Staniewska, K., Kowalik, J. (2021). The effect of triacylglycerol and fatty acid composition on the rheological properties of butter. *International Dairy Journal*, *114*, art. no. 104913.
https://doi.org/10.1016/j.idairyj.2020.104913

41. Tarapata, J., Łobacz, A., Żulewska, J. (2021). Physicochemical properties of skim milk gels obtained by combined bacterial fermentation and renneting: Effect of incubation temperature at constant inoculum level. *International Dairy Journal*, *123*, art. no. 105167.
https://doi.org/10.1016/j.idairyj.2021.105167

42. Tomaszewska-Gras, J. (2012). Detection of butter adulteration with water using differential scanning calorimetry. *Journal of Thermal Analysis and Calorimetry*, *108*, 433–438.
https://doi.org/10.1007/s10973-011-1913-y

43. Tomaszewska-Gras, J. (2013). Melting and crystallization DSC profiles of milk fat depending on selected factors. *Journal of Thermal Analysis and Calorimetry*, *11*3, 199–208.
https://doi.org/10.1007/s10973-013-3087-2

44. Truong, T., Bansal, N., Sharma, R., Palmer, M., Bhandari, B. (2014). Effects of emulsion droplet sizes on the crystallisation of milk fat. *Food Chemistry*, *145*, 725–735.
https://doi.org/10.1016/j.foodchem.2013.08.072

45. Viriato, R.L.S, de Souza Queirós, M., Neves, M.I.L., Ribeiro, A.P.B, Gigante, M.L. (2019). Improvement in the functionality of spreads based on milk fat by the addition of low melting triacylglycerols. *Food Research International*, *120*, 432–440.
https://doi.org/10.1016/j.foodres.2018.10.082